

Energy and isospin dependence of nuclear chaos

R. A. Molina, J. M. G. Gómez, and J. Retamosa

Departamento de Física Atómica, Molecular y Nuclear, Universidad Complutense de Madrid, E-28040 Madrid, Spain

(Received 23 July 2000; published 18 December 2000)

Energy levels and wave functions, obtained in realistic shell-model calculations for Ca and Sc isotopes up to $A=52$ and ^{46}Ti , are analyzed using standard statistics such as the nearest level spacing distribution, the Dyson-Mehta Δ_3 , and the mean localization length. These statistics are calculated for different energy regions of the spectrum. For all the Ca isotopes, in the ground state region the energy levels show strong deviations from Gaussian orthogonal ensemble predictions. It is shown that a transition to a more chaotic regime takes place as excitation energy increases. However, even when the full spectrum is taken into account, the Δ_3 and the degree of localization of the eigenfunctions in the mean-field basis prove that Ca isotopes are less chaotic than Sc isotopes. A comparison with ^{46}Ti shows that this nucleus is still more chaotic. Thus we find a clear isospin dependence in the degree of nuclear chaoticity.

DOI: 10.1103/PhysRevC.63.014311

PACS number(s): 21.60.Cs, 24.60.Lz

I. INTRODUCTION

Quantum chaos has made important progress during the last two decades. As far as stationary systems are concerned, the amount of compiled results shows a clear relationship between the fluctuation properties of the energy levels of a system and the large time scale behavior of its classical analog. The pioneering work of Berry [1], Bohigas *et al.* [2], and others leads to an important and concise statement: the spectral properties of simple systems known to be ergodic in the classical limit follow very closely those of the Gaussian orthogonal ensemble (GOE) of random matrices. In this case the distribution of the nearest-neighbor spacings is given to a good approximation by the Wigner surmise [3,4]. It corresponds to the existence of linear repulsion between adjacent levels. On the contrary, integrable systems lead to level fluctuations that are well described by the Poisson distribution, i.e., levels behave as if they were uncorrelated.

However, real and complex systems are usually not fully ergodic; neither are they integrable. The chaotic orbits only occupy a certain part of its phase space. There exist studies considering a class of Hamiltonians that depend on some parameters and whose behavior ranges from integrable to chaotic depending on the parameter values. When the system is quantized and its fluctuations studied, it is shown that the first neighbor distribution is progressively modified from Poisson- to Wigner-like. Intermediate cases where mixed statistics occur are well described by the Berry-Robnik [5] distribution. These intermediate situations are often described in terms of a single parameter by means of the Brody distribution [6], which is just an interpolation formula between the Poisson and Wigner distributions and has no obvious physical meaning.

The atomic nucleus can be considered as a small laboratory where the principles obtained in schematic systems may be tested. The information on regular and chaotic nuclear motion available from experimental data is rather limited, because the analysis of energy levels requires the knowledge of sufficiently large pure sequences, i.e., consecutive level samples all with the same quantum numbers (J, π, T) in a given nucleus. The situation is rather clear above the one-

nucleon emission threshold, where a large number of neutron and proton $J^\pi=1/2^+$ resonances are identified. The agreement between this Nuclear Data Ensemble (NDE) [7] and the GOE predictions is excellent. In the low-energy domain, however, it is rather difficult (if not impossible) to get large enough pure sequences. For this reason, even if the data coming from different nuclei are conveniently scaled and gathered, the conclusions are less clear. There is some evidence that, at low energy, the spectral fluctuations are close to GOE predictions in spherical nuclei while they deviate towards the Poisson distribution in deformed nuclei [8–11].

In order to get a deeper understanding of what happens in the low-energy region we can use the shell model with configuration mixing. Since the nucleus has no classical limit, there is no rigorous interpretation of regular or chaotic nuclear motion. One can, however, distinguish an approximate independent particle motion from the true correlated particle motion. In spherical nuclei, the nuclear shell model has been very successful in the description of low-energy nuclear states. This model is based on the existence of a symmetric mean-field potential which gives rise to single-particle states characterized by several good quantum numbers. This picture is destroyed by the strong nuclear residual interaction, leading normally to a chaotic nuclear motion. However, the perturbation of the independent particle motion is expected to be less effective in the ground state region where the level density is much lower than at higher energies.

Realistic shell-model calculations have shown that the *sd* shell nuclei show a strong chaotic behavior [12–14]. In the *pf* shell nuclei, however, the situation seems to be more interesting. In two previous papers [15,16] the spectral properties of the Ca isotopes and the $A=46$ isobars were studied. It was found that in the low-energy domain the Ca isotopes did not follow the GOE predictions. Moreover, the simple addition of a proton led to spectral fluctuations compatible with the GOE. Thus in this region of the nuclear chart it becomes possible to study with realistic shell-model calculations how nuclei evolve from quasiregular to chaotic motion as a function of isospin and excitation energy.

In this paper we present a detailed study of the energy

level and wave function statistics of ^{46}Ti and the Ca and Sc isotopes from $A=46$ to $A=52$. We calculate three statistics: (a) the nearest-neighbor level distribution $P(s)$, associated to short-range energy level correlations; (b) the Δ_3 introduced by Dyson and Mehta [17], which measures the departure of the spectrum from uniformity and is mainly related with long-range level correlations [12,18]; and (c) the localization length l_H [19], which is related to the complexity of the wave functions. The large shell-model spaces involved, with full diagonalization of matrices with dimensions up to 6107, provide reliable values for these statistics. We shall see how an order to chaos transition takes place as the excitation energy increases in Ca isotopes. A similar, but more abrupt transition takes place as one or two neutrons are replaced by protons in these nuclei, showing the existence of a clear isospin dependence in the degree of nuclear chaoticity.

The paper is organized as follows: First, the model, i.e., the valence space, the interaction, the unfolding method, and the three statistics $P(s)$, Δ_3 , and l_H , are briefly presented in Sec. II. Then, the results for these statistics in Ca, Sc, and Ti isotopes are discussed in Sec. III. Finally, we summarize the conclusions in Sec. IV.

II. BASIC FORMULAS

We follow the shell-model procedure to obtain the low-energy levels for a given nucleus. The most bound particles are assumed to form an inert core while the remaining nucleons move in a few single-particle orbits, the so-called valence space. For the lower part of the pf shell it is usual to take a core of ^{40}Ca and a valence space made of the $f_{7/2}$, $p_{3/2}$, $f_{5/2}$, and $p_{1/2}$ shells. We extract the single-particle energies from experiment and the residual two-body interaction is a monopole improved version of the Kuo-Brown interaction called KB3 [20]. The construction and subsequent diagonalization of the JT matrices was carried out using the code NATHAN [21] in an Alpha 500au workstation.

Fluctuations are somehow defined as the departure of the actual level density from a local uniform density. For this reason, and because of the exponential-like increase of the nuclear density, it is essential to eliminate this secular variation. There are several methods to map the actual spectrum onto a quasiuniform spectrum. We introduce a mean level density $\bar{\rho}(\alpha, E)$, where α stands for some parameters defining the functional form of the density. The mean cumulated level density is

$$\bar{N}(\alpha, E) = \int_0^E \bar{\rho}(\alpha, E') dE'. \quad (1)$$

The α optimal value α_0 is obtained minimizing the ‘‘distance’’

$$G(\alpha) = \int_{E_{min}}^{E_{max}} [N(E) - \bar{N}(\alpha, E)]^2 dE, \quad (2)$$

where $N(E)$ is the actual number of levels with energies less than or equal to E , and E_{min} and E_{max} are taken as the first and last energies of the level sequence. It is easy to show that

the ‘‘unfolded energy levels’’ $\{e_i = \bar{N}(E_i, \alpha_0)\}_{i=1,d}$ constitute a quasiuniform spectrum. Here d is the dimension of the given JT matrix.

It has been known, since the pioneering work of Mon and French [22], that the smoothed level density $\bar{\rho}$ for n nucleons in a major shell interacting via one- plus two-body forces has asymptotically Gaussian form. Sometimes Edgeworth corrections are added to improve the agreement between the smoothed and actual level densities, especially at the spectrum edges. Therefore, when the full spectrum or an appreciable part of it has been calculated, we take

$$\bar{\rho}(E) = \frac{d}{\sqrt{\pi A(1+BE_0)}} \exp\left(-\frac{(E-E_0)^2}{A^2}\right) (1+BE), \quad (3)$$

as a reasonable approximation to the true shell-model density [13], where E_0 , A , and B are the α set we must fit in order to minimize the distance (2).

When we want to analyze the low-energy part of the spectrum or when dimensionalities are so large that we only can obtain a small fraction of the energy levels, we describe the mean level density by the constant temperature formula [10]

$$\bar{\rho}(E) = \frac{1}{T} \exp[(E-E_0)/T], \quad (4)$$

where the constants T and E_0 are taken as parameters.

The distribution $P(s)$ of the nearest-neighbor spacings, $s_i = e_{i+1} - e_i$, is the best statistic to study the short-range correlations in the level spectrum. It is obtained by counting the spacings s_i that lie in a certain interval $[s, s+\Delta s]$ and normalizing the resulting distribution. To quantify the chaoticity of $P(s)$ in terms of a single parameter ω , we fit it to the Brody distribution [12]:

$$P(s, \omega) = \beta(\omega+1)s^\omega \exp(-\beta s^{\omega+1}),$$

$$\beta = \left[\Gamma\left(\frac{\omega+2}{\omega+1}\right) \right]^{\omega+1}. \quad (5)$$

Although it has no obvious physical meaning, the interesting feature of this distribution is that it interpolates between the Poisson distribution ($\omega=0$) and the Wigner distribution ($\omega=1$). The true GOE nearest-neighbor spacing distribution gives a fitted value ($\omega=0.953$) slightly smaller than the Wigner surmise. The ω value for which we obtain the best fit to the actual $P(s)$ is calculated using the least-squares method.

The long-range correlations between unfolded energy levels can be characterized by the Δ_3 statistic, defined for the interval $[a, a+L]$ in the cumulative unfolded level density as

$$\Delta_3(a, L) = \frac{1}{L} \min_{A, B} \int_a^{a+L} [N(e) - Ae - B]^2 de. \quad (6)$$

TABLE I. Nuclei, J values, and number of energy spacings for the different cutoff energies included in the calculations. Only $T=T_z$ states are considered.

Nucleus	⁴⁶ Ca	⁴⁸ Ca	⁵⁰ Ca	⁵² Ca	⁴⁶ Sc	⁴⁸ Sc	⁵⁰ Sc	⁵² Sc	⁴⁶ Ti
J	0-12	0-12	0-12	0-12	0-12	0-4, 7-12	0-1, 9-12	0, 11, 12	0-5, 8-12
$E < 5$ MeV	96	128	140	133	155	173	120	55	77
$E < 10$ MeV	441	654	818	658	1050	1328	950	405	553
All E	3937	11981	17203	11981	25498	14207	8031	11493	4508

Thus it measures the deviations of the quasiuniform spectrum from a true equidistant spectrum. To calculate Δ_3 as a function of the length L we follow the method explained in Ref. [2].

The complexity of a normalized state $|\alpha\rangle$ can be measured by means of the information entropy [23]

$$I_H(|\alpha\rangle) = \sum_{i=1}^d -|w_i^\alpha|^2 \ln(|w_i^\alpha|^2), \quad (7)$$

where w_i^α is the set of amplitudes of this state in the mean-field basis. For any state of the basis $I_H=0$, and it takes its maximum value, $\ln(d)$, for a uniformly distributed state. Obviously, there cannot exist many states with all their components nearly equal to $1/d$. Orthogonality and also symmetries like rotational and time-reversal invariance give rise to a smaller average value. For GOE matrices $\langle I_H \rangle = \ln(0.48d)$ [12]. The information entropy I_H measures, somehow, the degree of delocalization of a certain state with regard to the mean-field basis. However, its dependence on the dimension d of the matrix raises a problem when we are comparing states with different $J^\pi T$. In order to circumvent this problem the normalized localization length [19] has been introduced as

$$l_H = \frac{\exp(I_H)}{0.48d}. \quad (8)$$

To avoid strong fluctuations from one state to another, a mean localization length is defined [24],

$$\langle l_H \rangle = \frac{\exp(\langle I_H \rangle)}{0.48d}, \quad (9)$$

where $\langle I_H \rangle$ is obtained averaging the entropy over all the eigenstates of a given $J^\pi T$ matrix.

III. CHAOTICITY OF Ca AND Sc ISOTOPES: ANALYSIS OF THE $P(s)$, Δ_3 , AND l_H STATISTICS

Recently [15,16] we studied the spectral fluctuations of the Ca isotopes in the low-energy domain and significant discrepancies with GOE predictions were found. However, other $A=46$ nuclei such as ⁴⁶Sc, ⁴⁶Ti, and ⁴⁶V showed a clear chaotic behavior in the low-energy region. It was suggested, as a plausible explanation, that because of its larger strength, the proton-neutron interaction disturbs the regular mean-field motion more than the neutron-neutron interaction does. In order to verify this effect we have performed a de-

tailed comparative analysis of spectral properties and wave functions of the $A=46, 48, 50,$ and 52 Ca and Sc isotopes and ⁴⁶Ti. To get information on the T dependence for a given mass number A , it is sufficient to study the $T=T_z$ states in all the cases. The dimensions of the shell-model $J^\pi T$ matrices involved are very large, up to 36287. We have made a selection of J matrices in which a full diagonalization could be performed, including up to dimension 6107 for the $J^\pi T=0^+5$ states of ⁵²Sc. For some larger J spaces in ⁴⁸Sc, ⁵⁰Sc, and ⁵²Sc only some thousand energy levels and wave functions were calculated.

The spectral fluctuations are measured by means of the two statistics $P(s)$ and Δ_3 described in Sec. II. To get a deeper understanding of the statistical properties of these nuclei we have also studied the behavior of the wave functions analyzing the localization length l_H . The first neighbor spacing distribution $P(s)$ has been studied including all the levels up to 5 MeV and 10 MeV above the yrast line and without any cutoff. In the first case the mean level density (3) was used to unfold the spectrum, while Eq. (5) was employed in the other two cases. The unfolding is performed for each $J^\pi, T=T_z$ pure sequence separately and then the unfolded spacings are gathered into a single set for each nucleus to get better statistics. Table I shows the different J matrices considered for each nucleus and also the total number of spacings included, depending on the energy limit. Obviously the number of spacings increases quickly with the energy cutoff and with the number of active particles, and for the full energy spectrum the large number of spacings provides excellent statistics, ranging approximately between 4000 and 25 000 spacings per nucleus.

The values of the Brody parameter are displayed in Fig. 1 separated in three subpanels according to the energy cutoff. Figures 2–4 compare the $P(s)$ distributions of Ca and Sc isotopes for $A=48, 50,$ and 52 , depending on the energy cutoff. Up to 5 MeV above the yrast line, Ca isotopes show spectral fluctuations intermediate between those of regular and chaotic systems, except ⁵²Ca which essentially is a regular system. On the contrary, all the Sc isotopes and ⁴⁶Ti are very close to GOE fluctuations. For a given A , the big differences between Sc and Ca isotopes must be due to the residual two-body interaction, because the single-particle energies are the same in both cases. In Ref. [16] the results for $A=46$ were introduced and it was argued that the neutron-neutron force is much weaker than the neutron-proton force and thus the central field motion is less affected in the former case.

Another interesting feature observed in Fig. 1 is that the

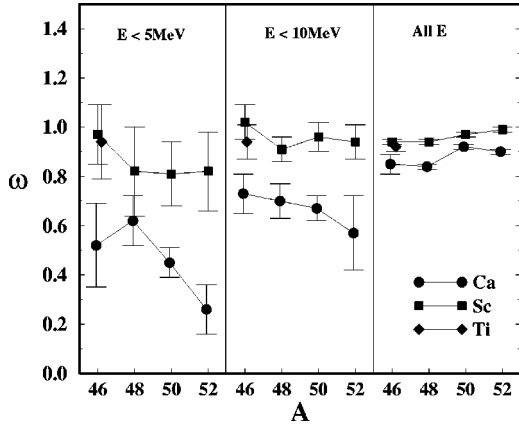


FIG. 1. Brody parameter ω for the $A = 46, 48, 50,$ and 52 Ca and Sc isotopes and ^{46}Ti , using all the energy levels up to 5 MeV and 10 MeV over the yrast line, and the full spectrum.

parameter ω for the Ca isotopes shows a strong fall from $A = 48$ to $A = 52$, where $\omega = 0.25$. It can also be observed looking at Fig. 2. As we go down from the top left to the bottom left panel, the Brody line moves away from the Wigner curve and progressively approaches the Poisson line. This astonishing result means that two-body interaction is almost unable to perturb the single-particle motion in the low-energy levels of ^{52}Ca . The large slope of ω as a function of A raises the

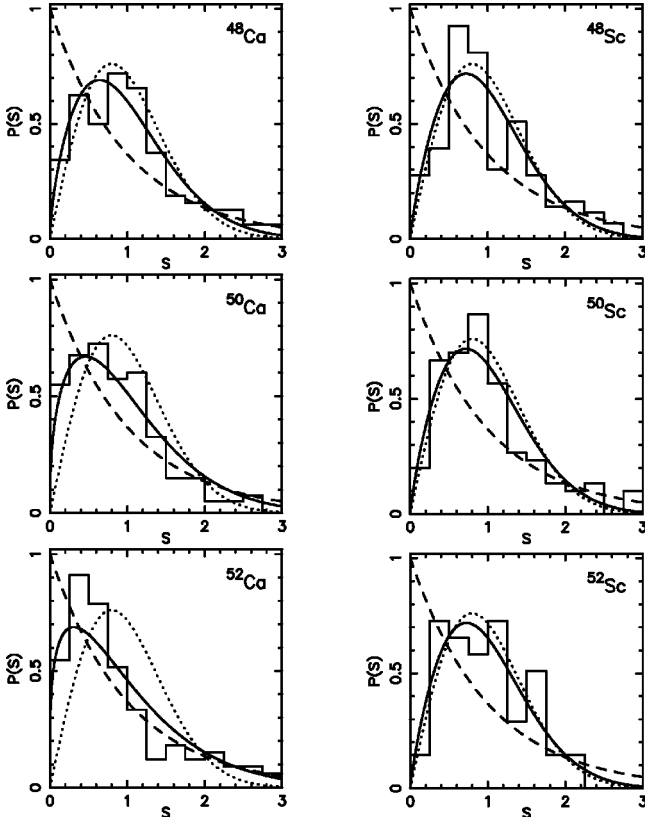


FIG. 2. Distribution of nearest-neighbor spacings $P(s)$ for Ca and Sc energy levels up to 5 MeV over the yrast line. The dotted, dashed, and solid curves stand for the GOE, Poisson, and best fit Brody distributions, respectively.

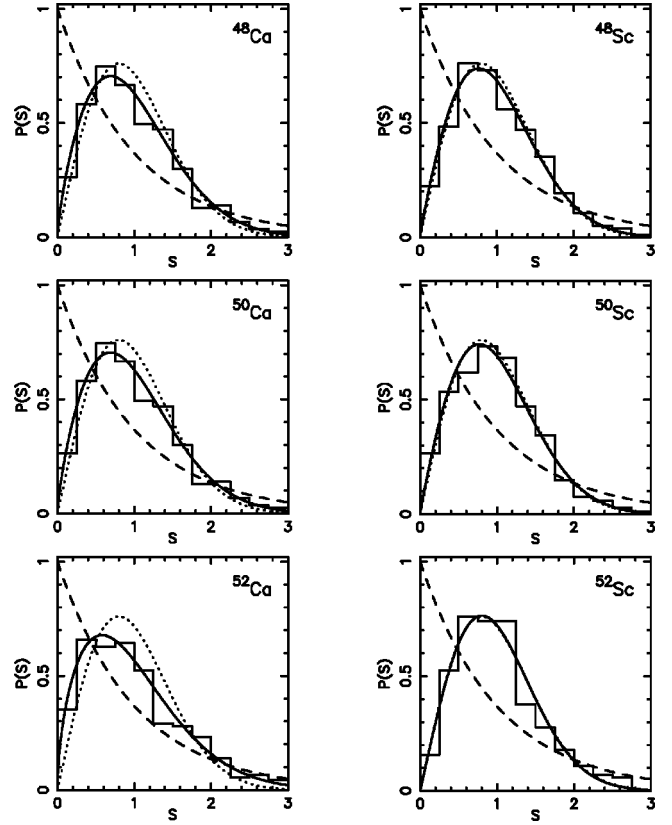


FIG. 3. Same as Fig. 2, but setting the energy cutoff at 10 MeV.

question why spectral fluctuations are so different in ^{48}Ca and ^{52}Ca . Actually, in our description, both nuclei are related to each other by a particle-hole transformation. Therefore, if the former nucleus consists of eight particles, the latter can be viewed as eight holes evolving in the pf shell. As the particle-particle and hole-hole interactions are identical, the observed differences can only be due to the central field. If we call ε_j the single-particle energies and $\bar{\varepsilon}_j$ the corresponding single-hole energies, it can be shown that

$$\bar{\varepsilon}_j = \varepsilon_0 - \varepsilon_j + \frac{1}{2j+1} \sum_k \sum_{(J)} \frac{2J+1}{1+\delta_{j,k}} V_{jkjk}^{J,T=1}, \quad (10)$$

where ε_0 is a constant given by

$$\varepsilon_0 = \sum_j (2j+1)\varepsilon_j + \sum_{j \leq k} \sum_{(J)} (2J+1)V_{jkjk}^{J,T=1}, \quad (11)$$

with $j, k \in \{7/2, 5/2, 3/2, 1/2\}$, and (J) means that the sum is restricted to angular momenta allowed by the Pauli principle.

The single-particle and single-hole pf spectra are compared in Fig. 5. The gaps between adjacent single-hole levels are in general larger and therefore in this case single-hole motion is less disturbed by the residual interaction than single-particle motion. Thus the combined effect of the weak neutron-neutron residual interaction and the large gaps in the single-hole energies seems to be the reason why the spectral fluctuations of the lower states of eight holes in the pf shell follow rather closely the Poisson distribution.

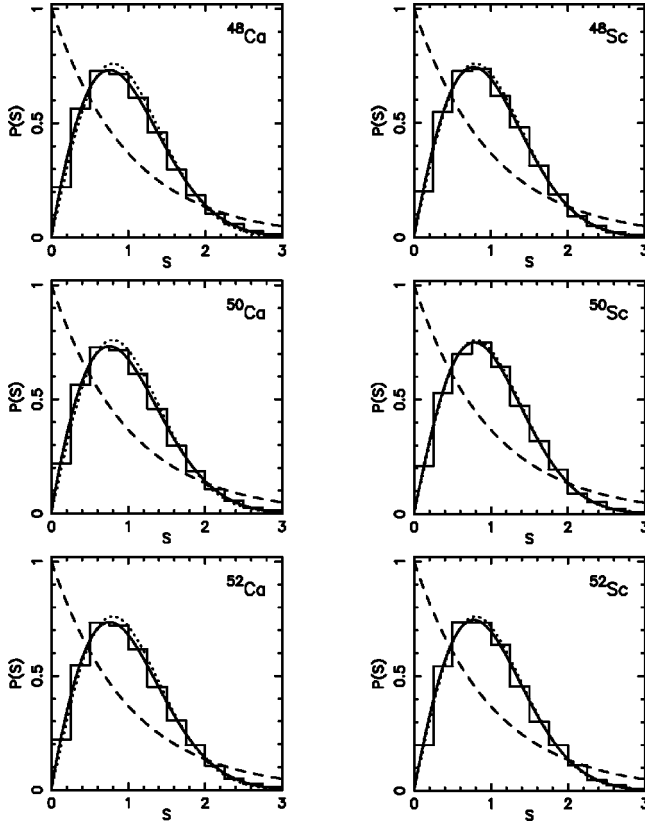


FIG. 4. Same as Fig. 2, but using the whole energy level spectrum.

As we go up in the energy spectrum, the new states become more and more complex combinations of many different configurations and thus the details of the one-body Hamiltonian will become progressively less important. When the energy cutoff is set at 10 MeV over the yrast line, there still exists a clear difference between the short-range level correlations of the two isotope sets. Comparison of Figs. 2 and 3 shows that Ca isotopes become more chaotic at 10 MeV than at 5 MeV, but the $P(s)$ at 10 MeV are still inter-

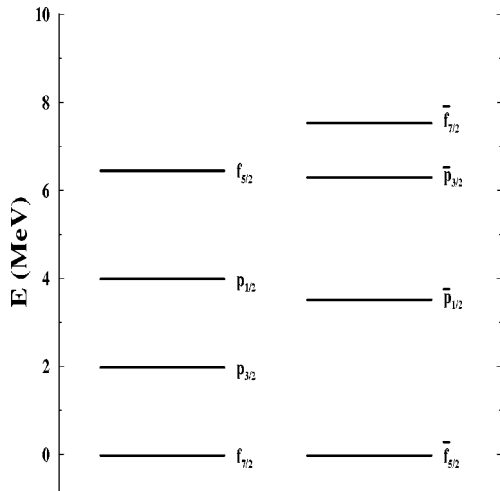


FIG. 5. Comparison of the single-particle and single-hole excitation energy spectra in the pf shell.

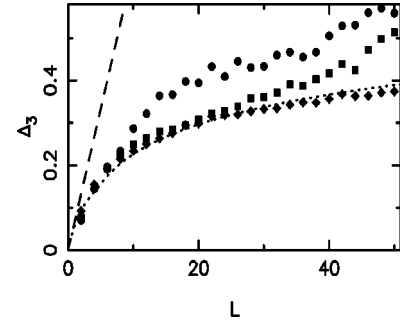


FIG. 6. Average Δ_3 for all the $J^\pi=0^+, T=T_z$ levels of ^{46}Ca (dots), ^{46}Sc (squares), and ^{46}Ti (diamonds). The dotted and dashed curves represent the GOE and Poisson Δ_3 values, respectively.

mediate between Poisson and Wigner distributions, while they are clearly Wigner like for Sc isotopes. In this 10 MeV region ω decreases smoothly from ^{48}Ca to ^{52}Ca , as Fig. 1 shows. Finally, when the whole energy spectrum is taken into account, the $P(s)$ distribution is dominated by the high-density central part of the spectrum and the Ca isotopes become almost fully chaotic systems. Because of the high level density at higher energies, the strong residual interaction mixes each independent-particle state with many other nearby states.

The ω value for ^{46}Ti has been included in Fig. 1 to show that, for all the energies, the Brody parameter already reaches its maximum for ^{46}Sc . Therefore, according to short-range level correlation behavior, replacing a single neutron by a proton in Ca isotopes causes a transition from a quasi-regular to a chaotic regime. It is remarkable that this transition takes place abruptly at all excitation energies in all the isotopes. A second replacement of a neutron by a proton does not seem to produce appreciable effects.

In order to confirm the previous results, we have computed the $\Delta_3(L)$ statistic for some $J^\pi, T=T_z$ sequences. To obtain the $\Delta_3(L)$ value for each L , we take its average value over many overlapping intervals of L unfolded spacings along the whole spectrum. Therefore, the results given below concern the full spectrum and not only the low energy region. Figure 6 shows $\Delta_3(L)$ values for $L \leq 50$, using the $J^\pi=0^+, T=T_z$ levels of ^{46}Ca , ^{46}Sc , and ^{46}Ti . Of the three nuclei, only ^{46}Ti follows the GOE line, at least until $L=50$. For ^{46}Sc the Δ_3 is close to GOE predictions up to a certain separation value $L_{sep} \approx 30$, where it unbends from the GOE curve. In ^{46}Ca the unbending starts at a smaller value $L_{sep} \approx 10$. In a chaotic system, Wigner level repulsion gives rise to a rigid spectrum, where long-range correlations are suppressed in comparison with a random sequence of levels. For such a system Δ_3 increases logarithmically following the GOE prediction. The unbending from the GOE curve and a linear growth of this statistic reveal a departure from the chaotic regime. This kind of behavior of the Δ_3 statistic was first seen in one-body systems like billiards [25,26] and then in shell-model calculations by several authors [13,27]. The values of L_{sep} differ from one case to another depending on the valence space or the effective interaction for reasons which are not fully understood as yet. But for the same interaction and configuration space, the Δ_3 behavior clearly

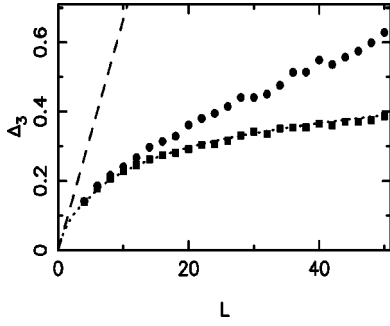


FIG. 7. Same as Fig. 6 for all the $J^\pi = 5^+, T = T_z$ levels of ^{52}Ca and ^{52}Sc .

shows a strong isospin dependence in the $A = 46$ nuclei, with chaoticity increasing as T decreases. This happens not only from Ca to Sc, but also from Sc to Ti. The same phenomenon is observed for other J values.

As another example, we compare in Fig. 7 the Δ_3 values for the $J^\pi = 0^+, T = T_z$ spectra of ^{52}Ca and ^{52}Sc . Here we see again that ^{52}Sc is clearly more chaotic than ^{52}Ca . Notice that in this case $L_{sep} > 50$ for ^{52}Sc , and comparing with Fig. 6 it seems to be more chaotic than ^{46}Sc . The main reason may be that there are more proton-neutron interactions in ^{52}Sc .

Summarizing the analysis of the spectral fluctuations, there exists a clear excitation energy and isospin dependence in the chaoticity degree of nuclear motion. It increases from Ca to Sc and from Sc to Ti. It is observed not only in the ground state region, but along the whole spectrum. When the full spectrum is taken into account, the $P(s)$ distribution is not very sensitive to the isospin dependence, but the effect is clearly seen in the Δ_3 statistic.

We undertook the study of the wave functions to see if they also show the differences observed in the spectral fluctuations. To be more precise, we have calculated the averaged normalized localization length $\langle l_H \rangle$ for the $J^\pi = 0^+, T = T_z$ states of the Ca and Sc isotopes and ^{46}Ti . Because we calculate the mean value using the complete sequence of states, the results do not only concern a small energy region, but all the spectrum. It can be seen in Fig. 8 that there is a clear difference between the Ca and Sc chains of isotopes and, again, the results for ^{46}Sc and ^{46}Ti are rather similar. For all the Ca isotopes $\langle l_H \rangle \approx 0.2$, while it increases to $\langle l_H \rangle \approx 0.4$ for the Sc isotopes. A value of $\langle l_H \rangle = 1$ means that the wave functions of the system are GOE like and have thus maximum delocalization. The small $\langle l_H \rangle$ in Ca isotopes means that the states are mainly localized in a relatively small number of components. In Sc isotopes the wave functions are much more spread, although still far from the GOE limit.

The $\langle l_H \rangle$ values give only the average spreading of the whole set of eigenfunctions for fixed $J^\pi T$. However, l_H has a strong energy dependence. This can be seen in Fig. 9, where l_H is plotted as a function of excitation energy for the $J = 6$ states of ^{50}Ca and the $J = 1, T = 2$ states of ^{46}Sc . We have chosen this example because both spaces practically have the same dimension, 2051 and 2042, respectively. The shape is essentially Gaussian [28], and therefore the wave functions

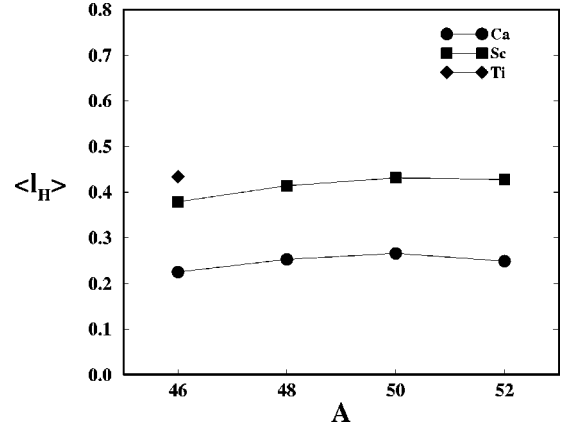


FIG. 8. Average localization length for the $J^\pi = 0^+, T = T_z$ states of several Ca and Sc isotopes and ^{46}Ti .

at the lower and upper edges of the spectrum are very localized, while $\langle l_H \rangle$ practically coincides with the l_H values in the central part of the spectrum, where the level density is much higher. Fig. 9 shows that even in the most chaotic central region of the spectra, the Ca are more localized than the Sc states. Since the space dimensions are almost the same in both cases, the differences in localization cannot be an spurious effect related to the space dimensions. These results are consistent with the spectral fluctuation results.

IV. DISCUSSION AND CONCLUSIONS

The spectral properties of experimental and theoretical nuclear energy levels have been studied by many authors and, in most cases where large pure level sequences are available, nuclear motion was found to be very chaotic. In the ground state region pure experimental sequences are short and the analysis is less reliable. There is some evidence of chaotic motion in spherical nuclei, especially in the light ones, while deviations towards regularity appear for deformed nuclei. But the available data are insufficient to establish border lines in mass number, excitation energy, an-

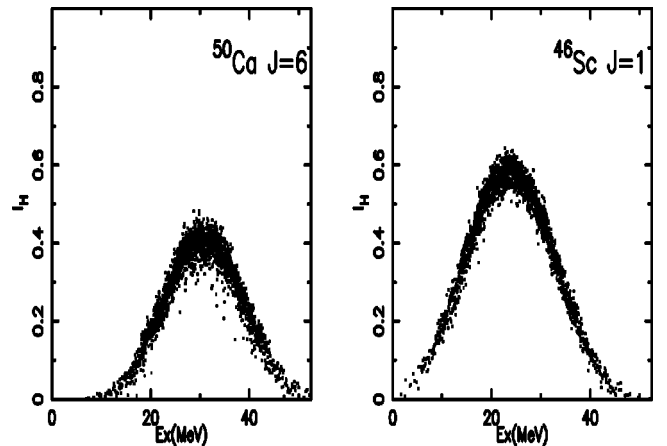


FIG. 9. Localization length as a function of excitation energy for the 2051 $J^\pi T = 6^+ 5$ states of ^{50}Ca and the 2042 $J^\pi T = 1^+ 2$ states of ^{46}Sc .

gular momentum, etc., between order and chaos in nuclei. Therefore, theoretical calculations are essentially the only tool to obtain that kind of information. All the shell-model calculations in the sd shell have shown that these light nuclei are very chaotic and thus they do not give insight into this problem. But the pf shell is more interesting in this context. As we have shown in this and previous papers, nuclear motion in the ground state region of Ca isotopes is intermediate between regular and chaotic, and in one of the isotopes it is essentially regular. Thus it has been possible to study the evolution of the chaoticity degree as a function of mass number, excitation energy and isospin.

We have studied the fluctuation properties of energy levels in terms of the $P(s)$ and Δ_3 statistics, and the wave functions in terms of the localization length l_H . The shell-model description of Ca isotopes involves only active neutrons and depends only on the single-particle energies and the residual neutron-neutron interaction. The short-range correlations of energy levels up to 5 MeV above the yrast line are far from the GOE limit. The Brody parameter ω falls from 0.6 in ^{48}Ca to 0.2 in ^{52}Ca . Thus there is a strong dependence on the number of active neutrons. The $P(s)$ analysis has also been performed for energy levels up to 10 MeV above the yrast line and for the whole energy spectrum. As we move up in energy, the chaoticity in Ca isotopes increases smoothly until $\omega \approx 0.9$.

In order to study if there is an isospin dependence, we made similar calculations for the $T = T_z$ states of Sc isotopes and ^{46}Ti . For all these nuclei and for all the excitation energy regions the short-range energy level correlations are close to GOE limit, although some increase with excitation energy is also observed. The variation of the ω values from Ca to Sc is always quite large, especially at low energies. Thus it seems that replacing a single neutron by a proton in Ca produces an abrupt order to chaos transition.

When the whole energy spectrum is taken into account, the ω values for Ca and Sc, are very similar, although slightly larger for Sc for all A . However, the behavior of the Δ_3 statistic is very different. The $\Delta_3(L)$ curve upbends from

the GOE limit from a certain L value which clearly increases for decreasing isospin T , both from Ca to Sc and from Sc to Ti.

The wave function analysis in terms of the localization length l_H shows clear differences between Ca and Sc isotopes as well. The Ca states are more localized than those of Sc in the mean-field basis. The difference is evident even in the central part of the energy spectrum, where the states are most chaotic. But even in this region the l_H values are far from the GOE value.

According to these results, it seems necessary to consider various statistics simultaneously to assess the degree of chaoticity of a quantum system like the nucleus. The combined analysis of the three statistics considered for Ca, Sc, and Ti isotopes reveals a smooth excitation energy dependence and a very sharp isospin dependence of nuclear chaoticity.

A possible interpretation of the isospin dependence is the effectiveness of the residual interaction in destroying the regular mean field motion. As is well known, the average neutron-neutron residual interaction is much weaker than proton-neutron one. Since Ca isotopes only involve active neutrons, the mean-field motion is less perturbed than in Sc and in Sc less than in Ti. Another possible explanation of the remarkably regular motion in Ca isotopes is the existence of an underlying symmetry, like the one related to seniority. Although seniority is a broken symmetry of the nuclear Hamiltonian, it is well known that it becomes almost a good quantum number for states in the $f_{7/2}$ shell. To the extent that seniority is a good quantum number, a $J^\pi T$ sequence of energy levels becomes a mixture of uncorrelated sequences of energy levels of different seniority. In that case there is no level repulsion between states of different seniority and the $P(s)$ distribution becomes intermediate between GOE and Poisson limits. These questions require further investigation.

ACKNOWLEDGMENTS

This work was supported in part by Spanish Government Grant No. DGES-PB96-0604.

-
- [1] M. V. Berry, *Ann. Phys. (N.Y.)* **131**, 163 (1981).
 - [2] O. Bohigas, M. J. Giannoni, and C. Schmidt, *Phys. Rev. Lett.* **52**, 1 (1984).
 - [3] E. P. Wigner, in *Proceedings of the International Conference on the Neutron Interactions with the Nucleus*, Columbia University, 1957, Columbia University Report No. CU-175, p. 49.
 - [4] L. D. Landau and Ya. Smorodinsky, *Lectures in Nuclear Theory* (Plenum, New York, 1965), Chap. 7, p. 69.
 - [5] M. V. Berry and M. Robnik, *J. Phys. A* **17**, L-831 (1984).
 - [6] T. A. Brody, *Lett. Nuovo Cimento Soc. Ital. Fis.* **7**, 482 (1973).
 - [7] R. U. Haq, A. Pandey, and O. Bohigas, *Phys. Rev. Lett.* **48**, 1086 (1982).
 - [8] G. E. Mitchell, E. G. Bilpuch, P. M. Endt, and J. F. Shrinier, Jr., *Phys. Rev. Lett.* **61**, 1473 (1988).
 - [9] J. F. Shrinier, Jr., E. G. Bilpuch, P. M. Endt, and G. E. Mitchell, *Z. Phys. A* **335**, 393 (1990).
 - [10] J. F. Shrinier, Jr., G. E. Mitchell, and T. von Egidy, *Z. Phys. A* **338**, 309 (1991).
 - [11] J. D. Garret, J. R. German, L. Courtney, and J. M. Espino, in *Future Directions in Nuclear Physics with 4th Gamma Detection Systems of the New Generation*, edited by J. Dudek and B. Haas, AIP Conf. Proc. No. 259 (AIP, New York, 1992), p. 345.
 - [12] T. A. Brody, J. Flores, J. B. French, P. A. Mello, A. Pandey, and S. S. M. Wong, *Rev. Mod. Phys.* **53**, 385 (1981).
 - [13] W. E. Ormand and R. A. Broglia, *Phys. Rev. C* **46**, 1710 (1992).
 - [14] M. Horoi, V. Zelevinsky, and B. A. Brown, *Phys. Rev. Lett.* **74**, 5194 (1995).
 - [15] E. Caurier, J. M. G. Gómez, V. R. Manfredi, and L. Salasnich, *Phys. Lett. B* **365**, 7 (1996).
 - [16] J. M. G. Gómez, V. R. Manfredi, L. Salasnich, and E. Caurier, *Phys. Rev. C* **58**, 2108 (1998).

- [17] F. J. Dyson and M. L. Mehta, *J. Math. Phys.* **4**, 701 (1963).
- [18] O. Bohigas and M. J. Giannoni, *Ann. Phys. (N.Y.)* **89**, 393 (1975).
- [19] F. M. Izrailev, *Phys. Lett. A* **134**, 13 (1988); *J. Phys. A* **22**, 865 (1989).
- [20] A. Poves and A. Zuker, *Phys. Rep.* **70**, 4 (1981).
- [21] E. Caurier, G. Martínez-Pinedo, F. Nowacki, A. Poves, J. Retamosa, and A. P. Zuker, *Phys. Rev. C* **59**, 2033 (1999).
- [22] K. K. Mon and J. B. French, *Ann. Phys. (N.Y.)* **95**, 90 (1975).
- [23] T. M. Cover and S. A. Thomas, *Elements of Information Theory* (Wiley, New York, 1991), p. 12.
- [24] F. M. Izrailev, *Phys. Rep.* **196**, 299 (1990).
- [25] P. Arve, *Phys. Rev. A* **44**, 6920 (1991).
- [26] H. D. Gräf, H. L. Harney, H. Lengler, C. H. Lewenkopff, C. Rangacharyulu, A. Richter, P. Schardt, and H. A. Weidenmüller, *Phys. Rev. Lett.* **69**, 1296 (1992).
- [27] V. Zelevinsky, B. A. Brown, N. Frazier, and M. Horoi, *Phys. Rep.* **276**, 35 (1996).
- [28] V. K. B. Kota and R. Sahu, *Phys. Lett. B* **429**, 1 (1998).